Energy 219 (2021) 119660

Contents lists available at ScienceDirect

Energy

journal homepage: www.elsevier.com/locate/energy

Experimental study on the off-design performances of a micro humid air turbine cycle: Thermodynamics, emissions and heat exchange

Zhen Xu [a, b, *], Yuan Lu [c], Bo Wang [c], Lifeng Zhao [c], Yunhan Xiao [c]

[a] School of Energy and Power Engineering, Shandong University, Jinan, Shandong, 250061, China
[b] Shandong Engineering Laboratory for High-efficiency Energy Conservation and Energy Storage Technology & Equipment, Shandong University, Jinan, Shandong, 250061, China
[c] Institute of Engineering Thermalphysics, Chinese Academy of Science, Beijing, China

ARTICLE INFO

Article history:
Received 2 March 2020
Received in revised form
20 October 2020
Accepted 17 December 2020
Available online 19 December 2020

Keywords:
Humid air turbine
Off-design performance
Emission
Thermodynamic

ABSTRACT

Micro humid air turbine (mHAT) is a promising distributed generation technology. However, the experiments, especially on the off-design characteristics, are still insufficient to support the theoretical model. In this paper, a detail experimental study is presented on a mHAT converted from a recuperated microturbine by introducing a humidifier, an aftercooler and an economizer. The steady-state thermodynamic performances, and the combustion and emission characteristics are evaluated at rated and part load condition. The off-design performances of the heat exchangers are also evaluated. It is shown that the specific output power and the electrical efficiency are relatively increased by 45% and 18.6% respectively comparing with the recuperated cycle at the rated load, and show a greater relative increment at part load, such as 58.1% and 21% respectively at 62.5% load. Introducing water into the air reduces the risk of NOx formation, but increases dramatically the risk of CO formation and incomplete combustion in the combustion chamber, thus the combustion efficiency deteriorates up to 92.5% at 50% of full load. The introduced heat exchange units display the characteristic of high effectiveness and low pressure loss, which is important for gas turbine system. The recuperator developed for the dry air also displays superior thermodynamic performance for the wet air with humidity ratio up to 0.108 $kg \cdot kg_{da}^{-1}$.

1. Introduction

With the worldwide growing of renewable energy power recently, new requirements of operation flexibility (such as faster load following and startup) and lower emission as well as high electrical efficiency have been put forward to traditional thermal power systems. Under this background, several advanced power cycle technologies based on gas turbine had been proposed and practiced. The most successful technology was Combined Cycle (CC) [1,2], but its load following capacity was delayed due to the steam turbine system and NOx emission was challenged by the increasing turbine inlet temperature. Humid Air Turbine (HAT), initially patented by Rao [3] in 1989, was another attractive technology for its better flexibility by canceling steam turbine and lower NOx emission by humid air combustion.

In last two decades, different HAT concepts were presented in open literature. Nakhamkin et al. [4] presented a cascade HAT concept to decrease the specific capital cost. Yan et al. proposed an externally fired HAT layout [5]. Ågren and Westermark proposed a HAT configuration in which a percentage of compressed intake air outlet bypassed the aftercooler and saturator [6]. This part-flow HAT had similar electrical efficiency with full-flow one, but higher system compactness and lower specific investment cost [7]. Dodo et al. proposed the Advanced Humid Air Turbine (AHAT) concept using the water atomizing inlet air-cooling (with overspray technology) to replace the intercooler between high- and low-pressure compressors [8]. More theoretical investigations were presented in Ref. [9–12]. The first HAT demonstration plant was converted from a simple-cycle gas turbine (VT600) in Lund University, and test result showed an efficiency increase from 22% to 35% at the rated power of 600 kW [13]. Hitachi built a 4MWe grade pilot plant to evaluate the AHAT concept that showed an electrical efficiency of 40% [14]. More recently, they further built a 40 MW grade AHAT system [15]. The tested cold startup time and NOx emission were 60 min and 24 ppm, respectively.

Although the HAT cycle has the highest efficiency for large-scale

* Corresponding author. School of Energy and Power Engineering, Shandong University, No.17923, Jingshi Road, Jinan, Shandong, 250061, China.

https://doi.org/10.1016/j.energy.2020.119660
0360-5442/

industrial turbines [16], its layout cannot be explained directly to a microturbine equipped with the single-stage compressor. Parente et al. proposed the micro Humid Air Turbine (mHAT) concept that distinguishes from the HAT by excluding the intercooler and aftercooler [17]. The mHAT exhibited excellent waste heat recovery and the rather limited modifications comparing to the commercial recuperated microturbine. De Paepe et al. [18] and Nikpey et al. [19] confirmed the potential of the mHAT by simulation of converting the Turbec T100 microturbine into a mHAT. De Paepe et al. further experimentally verified the mHAT concept by introducing a spray saturation tower with no internal packing into the Turbec T100 [20,21]. Wei and Zang developed a small-sized two-shaft HAT test loop without aftercooler and recuperator. First off-design experiment results were reported in Ref. [22]. However, installing an aftercooler may bring about additional benefit for the thermodynamics characteristics of mHAT. Thern et al. evaluated the impact of the aftercooler on the HAT pilot plant in Lund University. They reported a 1.5% and 0.4% increase of the air humidity and electrical efficiency, respectively [23]. Zhang and Xiao investigated the off-design performance of mHAT with aftercooler based on a simple cycle microturbine [24]. In our previous work, a mHAT test facility was built on an existing microturbines TG80, then the effect of aftercooler on the mHAT characteristics were experimentally evaluated. The result show an increase of 0.3% point when introducing the aftercooler in the simple mHAT layout [25]. All above authors had presented a significant electrical efficiency increase (~5% point), which depended on the machine size and cycle layout.

Though several experimental investigations had been carried out in the literature, the full operating characteristics (under rate output power and off-design conditions) of the mHAT, which could be used to verify the theoretical model, were still absent up to date. The purpose of this research is to present a detail test data of the mHAT layout considering a three-component heat exchanger network ($mHAT^{+}$ in Refs. [25]), which consists of two indirect heat exchanger (an aftercooler and an economizer) and an unconventional direct heat exchanger (humidifier). The experiments are conducted at the constant rotational speed. Within the output power range of full to 50%, the thermodynamic and emission performances of mHAT cycle and recuperated cycle are compared by maintaining the same turbine inlet temperature. The introduced heat exchanger units are evaluated by the effectiveness and pressure loss. The impacts of wet air operation on the original dry cycle components (the recuperator and the combustion chamber) are also discussed.

2. Experiment facility for mHAT

2.1. System layout

The mHAT is converted from an existing natural gas-fired microturbine (type TG80) with the single-stage centrifugal compressor and radial turbine. TG80 uses a constant rotation speed control strategy, which means the fuel flow, i.e., the Turbine Inlet Temperature (TIT), will be changed in variable load operation. The parameters of TG80 are listed in Table 1. Restricted by the generator structure and control system of porotype microturbine, the rated output power of mHAT is also set at the same 80 kW.

A three-component heat exchanger network (a humidifier, an aftercooler and an economizer) is integrated into TG80, while the original recuperator is not replaced, as shown in Fig. 1. There is no water recovery unit in this system. Thus, a two-stage reverse osmosis unit is introduced to provide the feed water. Converting an existing turbomachinery into HAT cycle, without redesigning original components, will bring several technical problems. The main ones are described as follows:

Table 1
Parameters of recuperated TG80 [26].

Parameter	Value
Ambient condition	1.013 bar, 15 °C, 60%RH
Inlet air mass flow[a]	0.73 kg s^{-1}
Pressure ratio	4.3
Rated electric power	80 kW
Electric efficiency	26%
Rotation speed	68000 r/m
Exhaust temperature	278 °C

[a] Measuring value.

(1) The imbalance of the flow going through the compressor and the turbine, caused by the air humidification (In the scale of microturbine, the volume flow rate of humid air in mHAT increases by more than 10% over the dry-air cycle), induces the risk of compressor surge and excessive shaft mechanical stress.
(2) Inserting a large volume after the compressor (humidifier) indeed increases the risk of compressor deep surge especially during the emergency shutdown [27] and has an impact on the transient behaviors of the system [28].
(3) Changing the composition of combustion air (i.e. adding high percentage of vapor into the air) may lead to flame instability and CO production in the combustor structure designed for dry air [29], and this factor can also affect the heat load of recuperator.
(4) The water loop in mHAT (see the solid line in Fig. 1) causes two problems: a cooperative control strategy is needed due to the introduction of two additional control parameters (the water flow rate through aftercooler and economizer), which are selected by the system simulation for mHAT. The water storage in the system should be considered to cope with the volume variation caused by evaporation and expansion on heating.

In our experiment facility, above mentioned problems have been discussed in design stage, and then some measures are adopted to minimize the threats to system operation:

- An air-bleed unit is equipped after the compressor, i.e., a part of air will be discharged in mHAT operation to balance the airflow in compressor and turbine, so that the risk of compressor surge is weakened.
- A compact humidifier based on a high-efficiency foam ceramic packing (the volume is only about 60% of traditional packing under the same conditions) is installed to reduce the influence of volume capacitance, and its bottom is enlarged to use as a water expansion capacity of 0.2 m^3 [30].
- An air bypass is established between the compressor and recupreator to switch dry- (recuperated) or wet- (mHAT) cycle as well as two water lines strategy, so that the impact of humidification on startup and shutdown process is weaken [31].
- A coordinated control system using a programmable logic controller is constructed to coordinate the output power adjustment of microturbine and humidification adjustment of heat exchanger network.

2.2. Heat exchanger network

The introduced heat exchanger network incorporates three additional components and a split water loop. In the layout, the

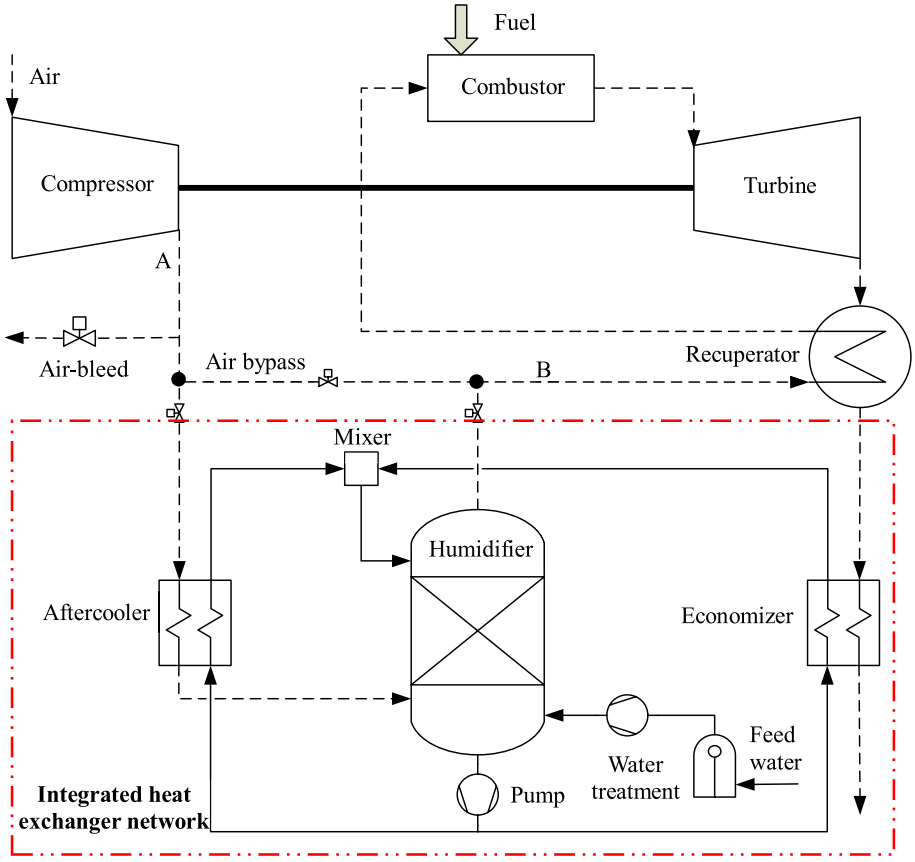

Fig. 1. Schematic of the mHAT experiment facility in this research.

split ratio of water stream plays an important role for the design of heat exchanger units since their inlet and outlet conditions strongly depend on the water flow rate through the aftercooler and the economizer. In order to determine the split ratio, the energy and mass balance of the whole cycle are analyzed and optimized using a simulation tool based on gPROMs. In this way, the selected design parameters of three heat exchange units are shown in Table 2, in which the humidity ratio is based on kg dry gas.

For waste heat recovery inside the cycle, the Outlet Water Temperature of Humidifier (OWTH) plays an important role. Although the lower OWTH is beneficial to waste heat recovery, the constraint condition of approach temperature (also be known as the pinch) should be paid more attention due to the requirement of compactness for humidifier. A smaller pinch will increase the size of humidifier, so a pinch of 5 °C is recommended for economic reason in the literature [32]. However, the improved heat and mass transfer capacity of foam ceramic packing used in our humidifier can broadens the selection range of pinch without the penalty of cost [30]. As a result, the pinch is selected to be 4 °C, and the corresponding OWTH is 5 °C above the wet bulb temperature of inlet air. Although low stack temperature is beneficial to waste heat recovery, it is still selected to be 90 °C (about 30 °C higher than the dew point) for the engineering requirements. In our mHAT facility, the exhaust pipeline (including indoor and outdoor parts) is about 30 m long, and a high exhaust superheat can effectively avoid condensation and corrosion.

Table 2
Design parameters of humidifier, aftercooler and economizer.

Parameter	Humidifier	Aftercooler	Economizer
Inlet water mass flow	0.86 kg s^{-1}	0.5 kg s^{-1}	0.36 kg s^{-1}
Inlet water temperature	109 °C	58 °C	58 °C
Outlet water temperature	62 °C	110 °C	108 °C
Inlet gas mass flow	0.73 kg s^{-1}	0.73 kg s^{-1}	0.79 kg s^{-1}
Inlet gas temperature	70 °C	218 °C	178 °C
Inlet gas humidity ratio	0.006 kg·kg_{da}^{-1}	0.006 kg·kg_{da}^{-1}	0.122 kg·kg_{df}^{-1}
Outlet gas temperature	86 °C	70 °C	90 °C
Outlet gas humidity ratio	0.099 kg·kg_{da}^{-1}	0.006 kg·kg_{da}^{-1}	0.122 kg·kg_{df}^{-1}

2.2.1. Humidifier

The humidifier is a direct heat exchanger, which adopts packed tower type with countercurrent arranged air and water stream. To simplify installation and maintenance, a flange connected three-segment structure is designed, as shown in Fig. 2. In the top segment, a perforated-ring-pipe water distributor and a stainless steel mesh mist eliminator are installed. In the intermediate section, a ceramic foam packing with height of 0.29 m is introduced. The air distributor is installed in the bottom segment, who is also used as the reservoir of water loop. At last, the humidifier developed for TG80 has a diameter of 0.55 m and a height of 2.28 m. More detail about the humidifier are reported in Ref. [30].

2.2.2. Aftercooler and economizer

Both the aftercooler and the economizer are used to transfer heat between the gas (pressured air in former and flue gas in latter) and the water, so the type of shell-and-tube heat exchanger (see Fig. 3 and Fig. 4) is selected. The water flows in the tube pass, and the gas flows in the shell pass. Since the convective heat transfer coefficient of the gas is much lower than that of the water, i.e., the shell-side thermal resistance is decisive to the heat transfer process

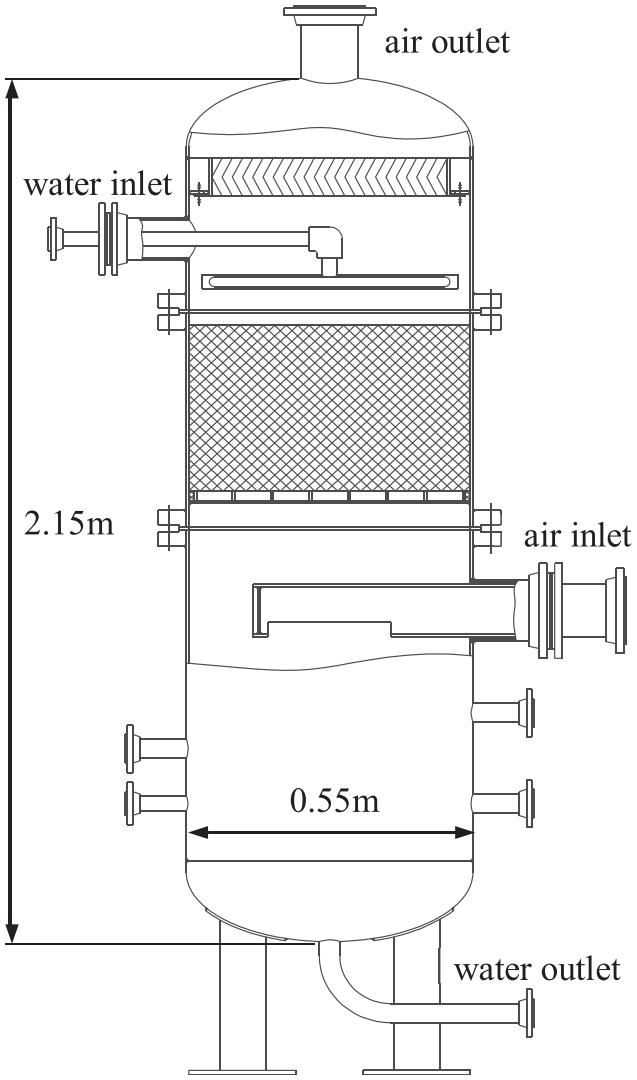

Fig. 2. Sketch of the humidifier.

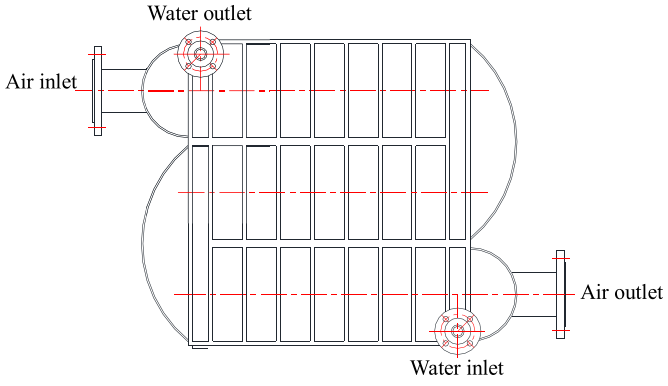

Fig. 3. Sketch of the three shell-pass aftercooler designed for mHAT.

between the water and the gas, the aluminum ring fins have been added to the tube outside surface to enhance the shell-side heat transfer. With the help of fins, the gas-water heat transfer area provided by the aftercooler and the economizer are 80 m^2 and 87 m^2, respectively. In addition, the aftercooler uses three shell-pass design to reduce the hydraulic diameter of gas path so that it can withstand higher gas pressure with shell as thin as possible.

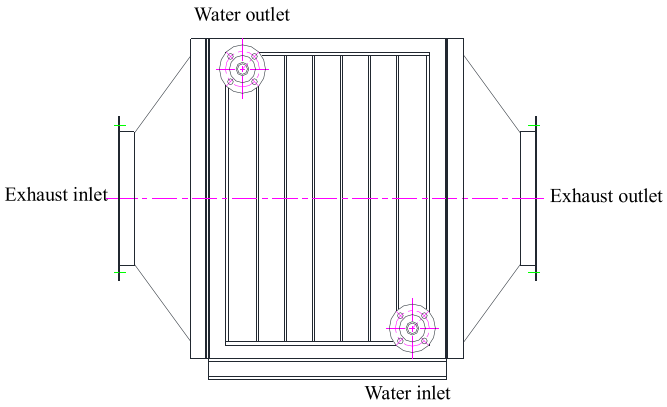

Fig. 4. Sketch of the one shell-pass economizer.

3. Experiment and evaluation approach

3.1. Thermodynamic performances

The experiments are operated at constant rotational speed and divided into two stage. At the first stage, the test facility starts up and increases to rated output power (80 kW) in Recuperated Cycle (RC) mode, and this process needs about 900 s to make the unit reach stable state. Then, the output power is reduced at 10 kW intervals to 50% of full load (40 kW). The transient process between two set point is about 60 s. Once the set point is reached, the measurement of thermodynamic and emission data is executed about 300 s. These results can be used as the reference to evaluate the performance of mHAT cycle. At the second stage, the test facility operates as a wet-cycle mode and the mHAT experiments are carried out at the same output power conditions. When adding water into the pressured air after the compressor as well as the resistance of aftercooler and humidifier, it is found that the air pressure at the outlet of compressor increases obviously. This increases the surge risk since the compressor characteristics of TG80 cannot be obtained to estimate its working point. On the other hand, when the output power is given, increasing the working fluid flow by humidification needs reduce the TIT within constrains of original microturbine control. To avoid compressor surge and adjust the TIT, air bleeding has been proved to be a good solution in mHAT operation. The mHAT experiments are carried out at the same TIT with RC. Since the TIT of microturbine can not be measured directly, the monitored Turbine Outlet Temperature (TOT) is corrected (based on the moisture content in the air) as an alternative.

The thermodynamic performances of mHAT are quantified by the Specific Output Power (SOP) and the Electrical Efficiency (EE). Since the compression work consumed by bleed air is not ignored, the SOP for mHAT should be defined as:

$$w = \frac{W_{net} + W_r - W_p}{m_{da}} \tag{1}$$

Where W_{net} is the net output power of the system; W_r is the compressing work of the bleed air; W_p is the pumping work consumed in the heat exchanger network; m_{da} is the mass flow rate of dry air. For RC, W_r and W_p are equal to zero, while for mHAT, W_p is calculated from the measured current and voltage, and W_r is decided by its ratio to the compressor power based on the measured air bleed flow rate.

Based on Eq. (2), the EE of cycles can be written as:

$$\eta = \frac{m_{da} w}{G Q_{LHV}} \tag{2}$$

Where G and Q_{LHV} are the standard volume flow rate and low heating value of the natural gas, respectively.

The low heating value, Q_{LHV}, is defined as the amount of heat released during an adiabatic combustion after the combustion products arrive at the same temperature and pressure at which the reactants enter. It can be given by:

$$Q_{LHV} = \sum_{j=1}^{n} \phi_j Q_{LHV,j} \tag{3}$$

Where n is the number of combustible composition in the natural gas; ϕ_j and $Q_{LHV,j}$ are the volume percentage and low heating value of composition j, respectively.

The compositions and their volume percentages of natural gas in our experiments are illustrated in Table 3. These data are obtained by sampling from the gas pipeline and testing in professional institutions. Using these data, the low heating value of natural gas can be calculated to be 36.6 MJ·Nm^{-3} by Eq. (3).

3.2. Performances of heat exchanger units

The potential performance benefits of a mHAT rely on the heat exchanger units, which could be divided into two types: the direct-contact exchanger (humidifier belongs to this type) and the indirect-contact exchanger (aftercooler, economizer and recuperator belong to this type). The thermodynamic characteristics of heat exchanger units are evaluated by the effectiveness and pressure loss coefficient.

For indirect-contact exchanger, the effectiveness is defined as the actual temperature change for the stream with lower capacity divided by the maximum possible change [33]:

$$\varepsilon = \frac{\max\left[(T_{c,o} - T_{c,i}), (T_{h,i} - T_{h,o})\right]}{T_{h,i} - T_{c,i}} \tag{4}$$

Where $T_{c,i}$, $T_{c,o}$, $T_{h,i}$, and $T_{h,o}$ are the inlet temperature of cold stream, outlet temperature of cold stream, inlet temperature of hot stream and outlet temperature of hot stream, respectively. The cold stream and hot stream in every indirect-contact exchanger of mHAT are shown in Table 4.

The effectiveness concept defined by Eq. (4) can not be directly translated to the direct-contact exchanger, i.e., the humidifier, due to the simultaneous mass and heat transfer in the air-water contact process. Therefore, the energy effectiveness concept is defined for the humidifier [34]:

Table 3
Natural gas compositions in the experiments.

Component	Molecular formula	Volume percentage
Methane	CH_4	94.63%
Ethane	C_2H_6	2.93%
Propane	C_3H_8	0.5%
N-butane and Isobutane	C_4H_{10}	0.18%
Pentane and Isopentane	C_5H_{12}	0.05%
Nitrogen	N_2	0.75%
Carbon dioxide	CO_2	0.96%

Table 4
Cold and hot stream in indirect-contact exchanger of mHAT.

Exchanger	Cold stream	Hot stream
Aftercooler	water	compressed air
Economizer	water	flue gas
Recuperator	compressed air	flue gas

$$\varepsilon = \frac{\Delta H}{\Delta H_{\max}} \tag{5}$$

Where ΔH and ΔH_{max} is the actual and maximum possible enthalpy rate difference, respectively.

The ΔH_{max} is decided by the heat capacity rate of the water stream or the air stream:

$$\Delta H_{\max,a} = m_{da}\left(h_{a,id}(T_{w,i}) - h_{a,i}\right) \tag{6}$$

$$\Delta H_{\max,w} = m_{w,i} h_{w,i} - m_{w,id} h_{w,id}(T_{wb}) \tag{7}$$

Considering the energy balance in the humidifier, the actual enthalpy rate difference of the water stream is the same as that of the air stream:

$$\Delta H_w = \Delta H_a = m_{da}\left(h_{a,o} - h_{a,i}\right) = m_{w,i} h_{w,i} - m_{w,o} h_{w,o} \tag{8}$$

Using Eq. (6)~(8), the energy effectiveness can be written as:

$$\varepsilon = \frac{\Delta H_a}{\min\left\{\Delta H_{\max,a}, \Delta H_{\max,w}\right\}} \tag{9}$$

The pressure loss coefficient of heat exchanger unit is defined as:

$$\beta = \frac{\Delta P}{P_f} \tag{10}$$

Where ΔP is the pressure loss caused by the heat exchanger unit, and P_f is the absolute pressure in the front of the heat exchanger unit.

3.3. Measurement method

The parameters measured in mHAT experiments include temperature, differential pressure, humidity, flow rate and concentration. The measurement method for these parameters are shown in Table 5.

In all the parameters, the humidity is very important for evaluating the performances of humidifier as well as the mHAT. The inlet air humidity of compressor is measured by the relative humidity sensor shown in Table 5, while the outlet air humidity of humidifier is difficult to be directly measured since the on-line relative humidity sensor could not work in saturated humid air. For the steady-state experiments, an alternative method is used by monitoring the water consumption over a period of time. In our present work, the magnetostrictive sensor with an uncertainty of ±1 mm and the turbine flowmeter are used to measure the bottom water level of humidifier and feed water flow rate respectively with a measuring period of 300s, then the water consumption can be calculated by these two parameters. In this way, a higher precision (about ±2%) can be obtained compared to on-line method.

Table 5
Measurement method and accuracy.

Parameter	Method	Range	Accuracy
Temperature	Pt100 RTD	0–500 °C	±0.5 °C
Differential pressure	capacitive sensor	0–10 kPa	±0.25% full scale
Relative humidity	hygrometer	0–100%	±1% full scale
Water flow rate	turbine flowmeter	0–3 m^3/h	±0.5% full scale
Air flow rate	vortex flowmeter	0–5000 m^3/h	±1% full scale
Concentration	flue gas analyzer	0–5000 ppm (NOx) 0–10000 ppm (CO)	±5% reading value

4. Results and discussion

4.1. Intake and exhaust condition

The intake temperature during the period of cycle experiments are illustrated in Fig. 5. It can be seen that the intake temperature change within the range of 12.5 °C–13.1 °C, respectively. At the same time, the air pressure and relative humidity at the compressor inlet is measured as 1.012 bar and 75%. As a result, the humid ratio of intake air can be calculated to be a constant of 0.007 $kg \cdot kg_{da}^{-1}$. Under this condition, the influence of intake parameters on RC and mHAT can be ignored when evaluating their thermodynamic performances.

The exhaust temperature and increased humidity ratio in the cycle experiments are shown in Fig. 6, in which the increased humidity ratio refers to the humidity ratio difference between the outlet and the inlet air stream of the humidifier. For all test conditions, the exhaust temperatures of mHAT are much lower than those of RC, but the corresponding humidity ratios increase significantly, which indicates that the sensible heat in flue gas is recovered and converted into latent heat of water vapor. In our present experiments, the maximal humidity ratio increment and exhaust temperature difference between RC and mHAT are 0.101 $kg \cdot kg_{da}^{-1}$ and 192 °C respectively. Both of them occur at full load condition and drop with decreasing load under the constant rotation speed control, as shows that less waste heat can be recovered when the mHAT operates at part load.

As mentioned in section 3.1, for the sake of comparison reference, the TIT instead of TOT should be keep the same in the experiments of RC and mHAT. This is because when a certain amount of water (by humidification and combustion) is introduced into the gas through the turbine, its decreasing specific heat ratio leads to lower temperature drop in the expansion process under the same pressure ratio, as shown in Fig. 7. In this Figure, the ΔTIT is the difference between TIT_{RC} and TIT_{mHAT}, where the TIT_{mHAT} with three humidity level are calculated based on the TOT_{RC}. It can be found that ΔTIT increases obviously with increasing gas humidity ratio at a rate of about 4–6 °C per 0.05 $kg \cdot kg_{df}^{-1}$ according to the set output power. In mHAT experiments, the maximum gas humidity ratio observed is about 0.133 $kg \cdot kg_{df}^{-1}$ at the rated load condition, corresponding to a ΔTIT of 16 °C, which has an impact of 0.4% points on the EE of mHAT.

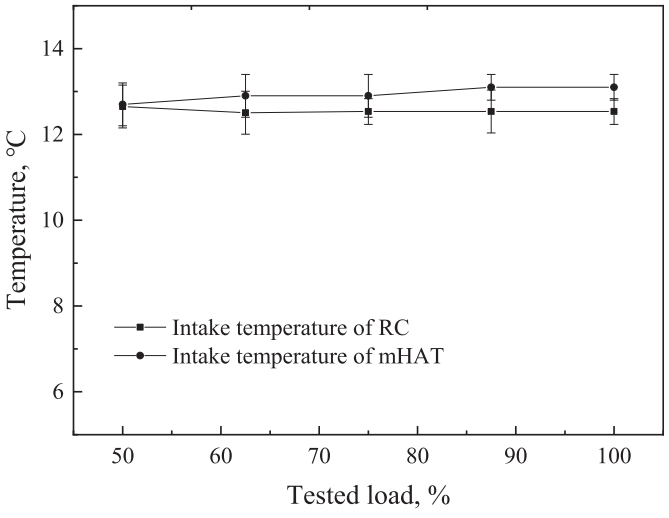

Fig. 5. Intake temperature in cycle experiments.

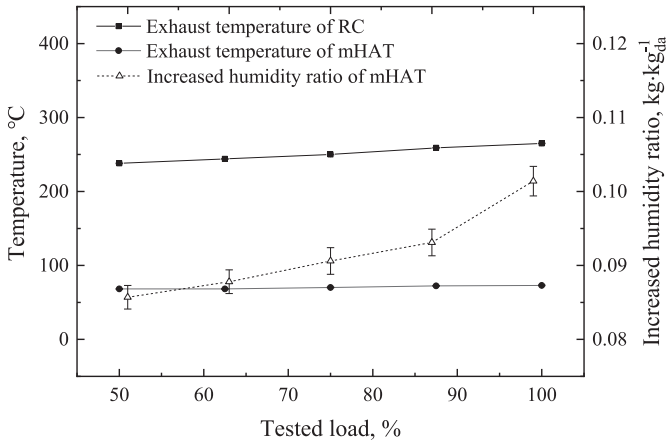

Fig. 6. Exhaust temperature and increased humidity ratio in cycle experiments.

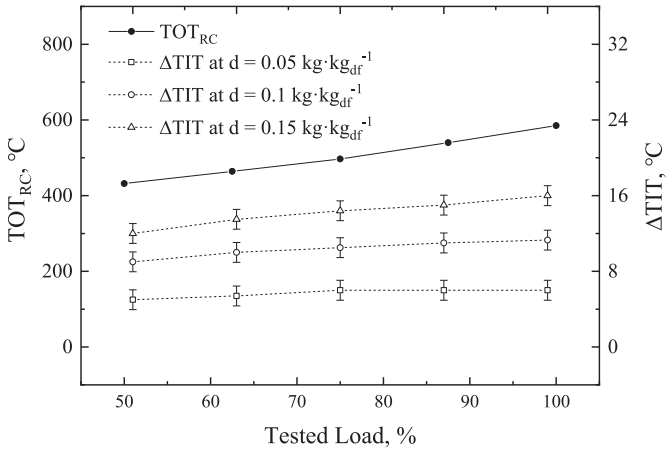

Fig. 7. Comparison of TIT at different humid ratio.

4.2. Specific output power and electrical efficiency

The SOP and EE of mHAT at rated and part load are shown in Fig. 8 and Fig. 9, respectively. The corresponding data of RC are also provided. It can be found that two cycles show similar trends in the thermodynamics performance, but the mHAT is vastly superior to the RC. At the rated load, the maximum SOP and EE are 109.1 kW kg^{-1} and 26.1% respectively for the recuperated microturbine, and these two parameters are relatively increase by 45% and 18.6% respectively for the mHAT. With decreasing load, the absolute values of SOP and EE decrease almost linearly, but theirs relative increments of mHAT to RC increase (such as 58.1% and 21% respectively at 62.5% of full load), i.e., even though the waste heat recovery reduces as seen in Fig. 6, the mHAT cycle is still more helpful to improve the part load performance of recuperated microturbine. From Fig. 8, it also can be seen the relative increment of EE drops dramatically when the load decreases below about 60%. This may be caused by the combustion efficiency reducing at off-design condition and more detail will be discussed in the next section.

4.3. Combustion and emission performance

When converting a dry cycle into wet cycle, one of the most attractive advantages is the NOx emission reduction due to the increased moisture content of combustion air in the combustion chamber [35–37]. For a microturbine, even though the NOx emission has been at a very low level, the introduction of water can allow to further reduce the risk of NOx formation, as seen in Fig. 10. At the rated load, the mHAT shows a maximum reduction of about 33% based on the 15 ppm NOx concentration in the exhaust of RC. The reduction of NOx emission benefits from the dilution effect of water vapor on oxygen content since the combustion temperature and pressure in the combustion chamber are the same for RC and mHAT. However, this effect is weakened by lower temperature (the combustion temperature decreases with decreasing load under constant rotational speed control) and lower humidifying capacity. When the load is reduced to 50%, the reduction of NOx decreases to 12.5%.

On the other hand, though the risk of NO_X formation could get lower, it is not true for the CO formation, as seen in Fig. 11. The experiments show that the CO emission increases significantly from 18 ppm to 161 ppm at rated load when converting TG80 into mHAT, and it is greatly impacted by decreasing load operation under the current control strategy. The maximum CO emission of

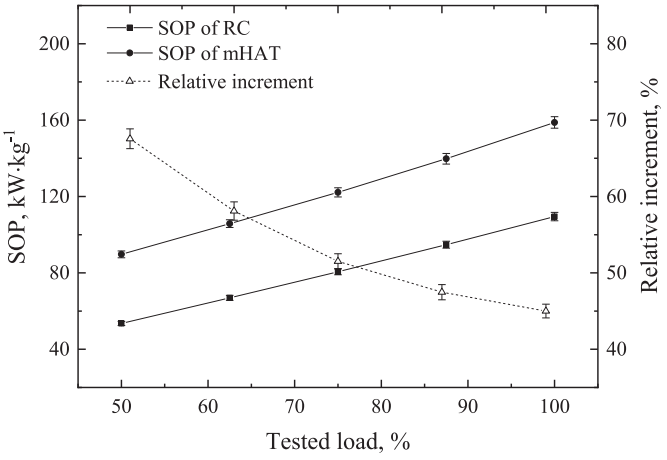

Fig. 8. Specific output power of RC and mHAT at different loads.

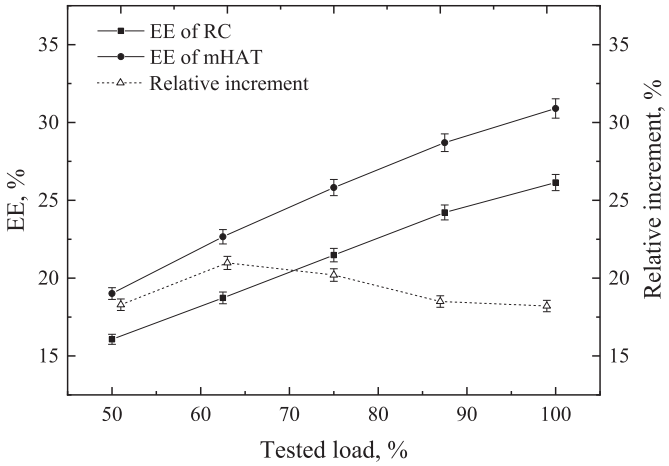

Fig. 9. Electrical efficiency of RC and mHAT at different load.

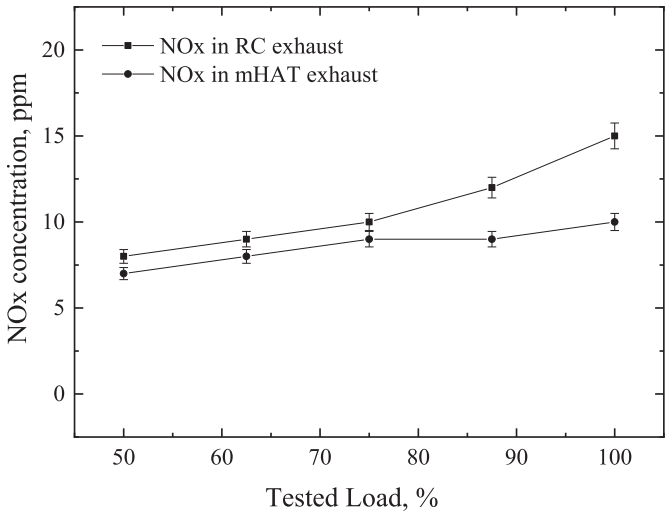

Fig. 10. NOx concentration in the exhaust of RC and mHAT at different load.

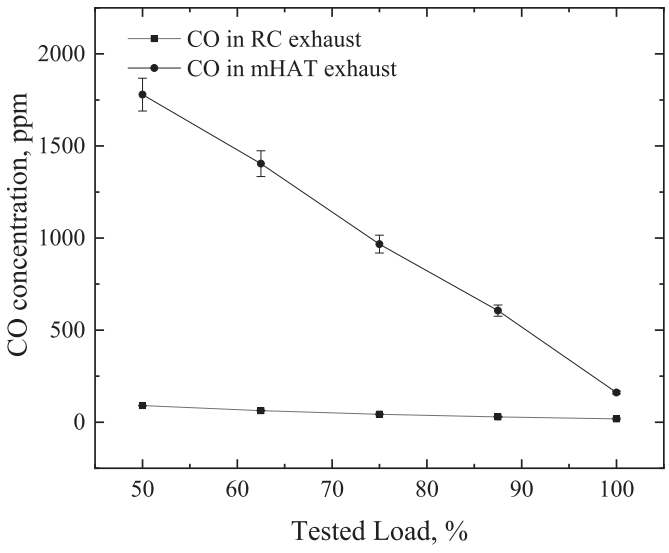

Fig. 11. CO concentration in the exhaust of RC and mHAT at different load.

mHAT obtained in the experiments is 1779 ppm comparing to only 90 ppm of RC at the 50% load. Generally, the CO emission is used as an index to evaluate the combustion efficiency in gas turbine, since introducing water into the pressured air beyond the allowable range of original dry air combustion chamber may cause risk of incomplete combustion. The very high CO emissions indicate the severe incomplete combustion at part load, which also is verified by the unburnt hydrocarbon (expressed as C_3H_8) measured in the exhaust. It is observed that the C_3H_8 of mHAT is 256 ppm comparing to 12 ppm of RC at the 50% load. Based on the measured data of flue gas and fuel compositions, the combustion efficiency of mHAT declines from 99.3% to 92.5% when the load changes from 100% to 50%, while the corresponding value of dry air operation is estimated to be above 99.5% in all conditions, as seen in Fig. 12. Obviously, the loss of combustion efficiency has a negative impact on the EE of mHAT, which can weaken the positive effect of air humidification. This explains the reason why the relative increment of EE appears inflection point with decreasing load in Fig. 9.

For the purpose of upgrading the existing microturbines into mHAT, the penalty of less than one percentage point decline in combustion efficiency is acceptable because the investment cost and modification difficult will be reduced. However, the adjustment of constant rotational speed control strategy should be considered to avoid its great threaten to the off-design behaviors of combustion chamber. When developing new microturbines based on mHAT cycle, an improved combustion chamber layout for wet-air operation is necessary.

4.4. Evaluation of heat exchanger network

As is known to all, gas-path pressure loss between the outlet of compressor and the inlet of combustion chamber has a considerable impact on the EE of microturbine [38]. Low pressure loss is an extremely important design principle for a heat exchange unit introduced into the gas-path. The effectiveness is also a significant factor as well as the pressure loss, since it can reflect the thermodynamic perfection degree of heat exchange process.

The pressure loss coefficient and effectiveness of introduced heat exchanger units in the mHAT are illustrated in Fig. 13 and Fig. 14, respectively. It can be found that all the three introduced heat exchanger units show excellent hydrodynamics and thermodynamics characteristics. The economizer shows a minimum pressure loss ($\beta = 0.28$) at the rated condition, but those of the aftercooler and humidifier are 0.48 and 0.6 respectively. For mHAT system, the latter two have a greater impact on EE since both of them are installed in the gas-path between the compressor outlet and combustion chamber inlet. However, of the best kind, the present design of aftercooler and humidifier only contributes a small share (about 19.5%) of flow resistance comparing to the whole gas-path between the compressor out and combustion chamber inlet, as seen in Fig. 13. Reducing the load of mHAT will slightly increase the pressure loss of the aftercooler and humidifier, but has little effect on the economizer. The effectiveness displays the similar trend as the pressure loss, i.e., is also not sensitive to the load changing condition. Among the three introduced heat exchanger units, the humidifier has the maximum exergy loss due to the couple heat and mass transfer occurring between the air and water, which could explain why the humidifier has the minimum effectiveness of 0.75 at the rated condition.

The recuperator plays an important role in the internal heat recovery whether for RC or mHAT. When converting the working fluid from dry air into wet air, significant changes in inlet air

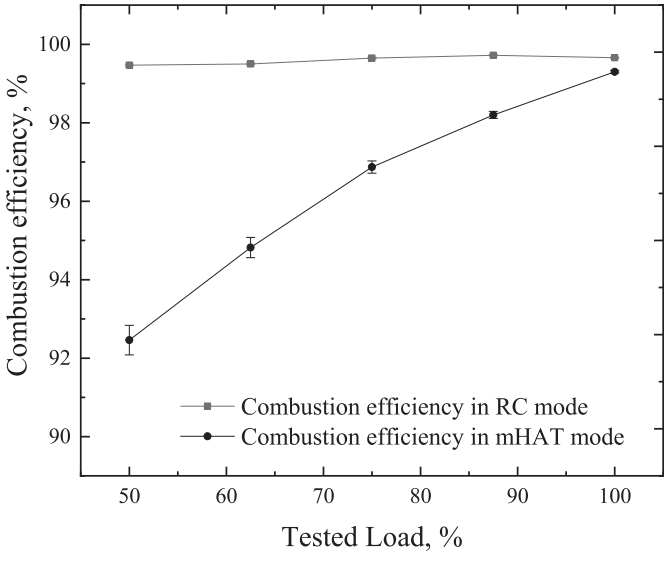

Fig. 12. Combustion efficiency in RC and mHAT experiments.

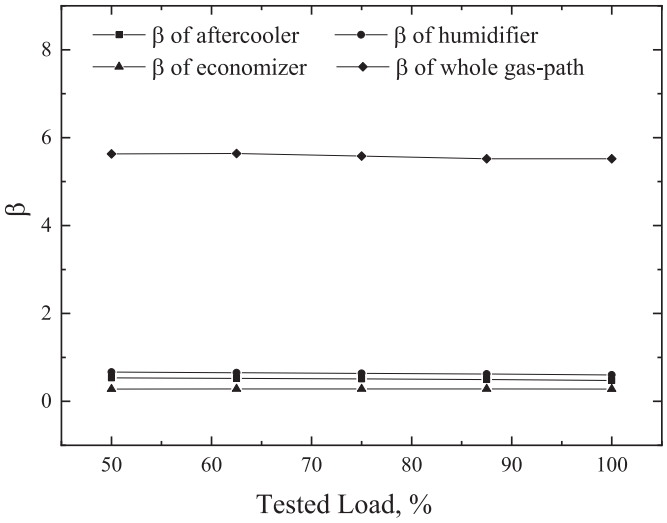

Fig. 13. Pressure loss coefficient of introduced heat exchanger units in mHAT.

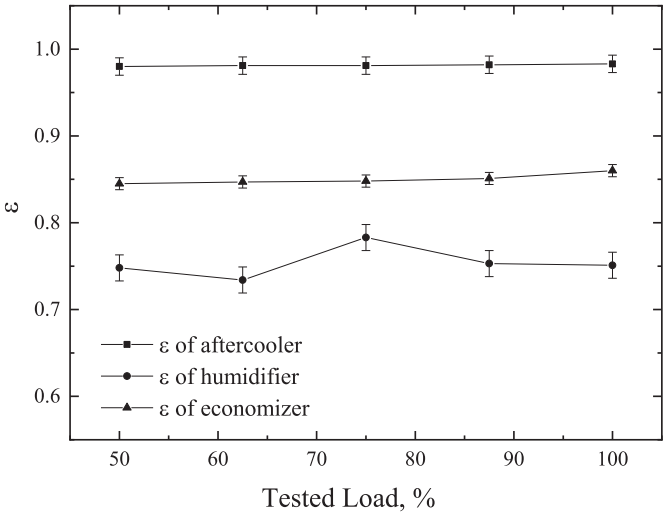

Fig. 14. Effectiveness of introduced heat exchanger units in mHAT.

temperature (see Fig. 15) and humidity (see Fig. 6) make the recupreator run under off-design condition, which usually has an impact on its thermodynamic performance. However, it can be found in Fig. 16 that the effectiveness of recuperator is as high as 0.9 in wet air operation and even slightly higher than that in original dry air operation at the full load condition. At the same time, the temperature difference between inlet and outlet air of recuperator increases about 120 °C, then the heat flux on the heat exchanging surface is improved remarkably, which can be attributed to the increased heat capacity rate of wet air since the water vapor has a twice higher of specific heat than the dry air, as shown in Fig. 17. According to the experiments, the recuperator developed for dry air is also acceptable for the wet air with humidity ratio up to 0.108 $kg \cdot kg_{da}^{-1}$ for the purpose of upgrading the existing micro-turbines, thus the cost and modification difficult will be significantly reduced.

5. Conclusion

In this paper, the experimental study on a mHAT cycle is carried out at the constant rotational speed and turbine inlet temperature. The test facility converts from a recuperated microturbine by introducing a three-component heat exchanger network, i.e. an aftercooler, an economizer and a humidifier. The steady-state performance of the system are checked in the changing output power range of full to 50%. The main conclusions are as follows:

(1) The mHAT cycle shows excellent steady-state performances on 100 kW grade microturbine. Comparing to the RC, the specific output power and the electrical efficiency increase 45% and 18.6% respectively at the rated load, and show a higher relative increment at part load condition. The outstanding off-design performances make the mHAT suitable for the application with high flexibility requirements such as combined heat and power (CHP) or cogeneration.

(2) Introducing water into the air reduces the risk of NOx formation in the combustion chamber, thus the impact of microturbine on the environment can be further decreased. However, under constant rotational speed control, the risk of CO formation and incomplete combustion in the combustion chamber increases dramatically with decreasing combustion temperature, and the corresponding combustion efficiency drops up to 92.5% at 50% load. As a result, an improved combustion chamber layout as well as system control strategy for wet-air operation is necessary when developing the mHAT technology.

(3) The introduced aftercooler, economizer and humidifier show the characteristic of high effectiveness and low pressure loss, which is important for gas turbine components and proves the applicability of our present design. The recuperator developed for the dry air operation also displays superior thermodynamic performance for the wet air with humidity ratio up to 0.108 $kg \cdot kg_{da}^{-1}$, thus it is also an acceptable options in the mHAT.

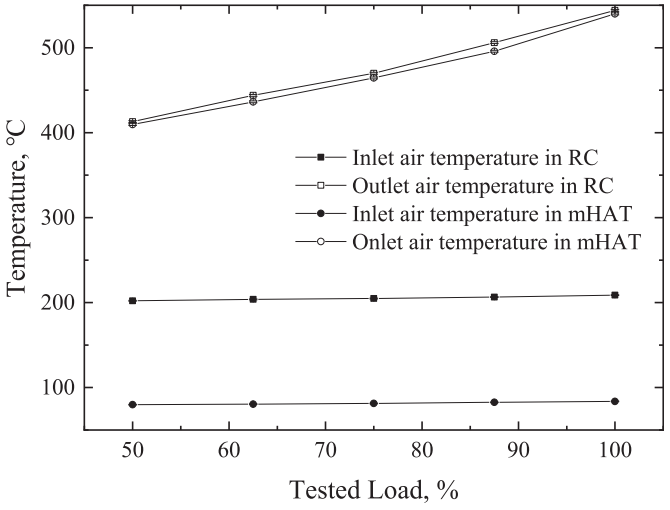

Fig. 15. Inlet and outlet air temperature of recuperator in RC and mHAT.

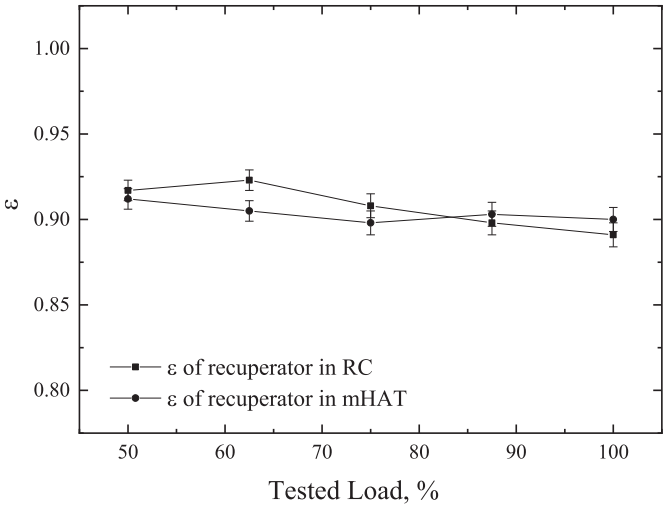

Fig. 16. Comparison of recuperator effectiveness in RC and mHAT.

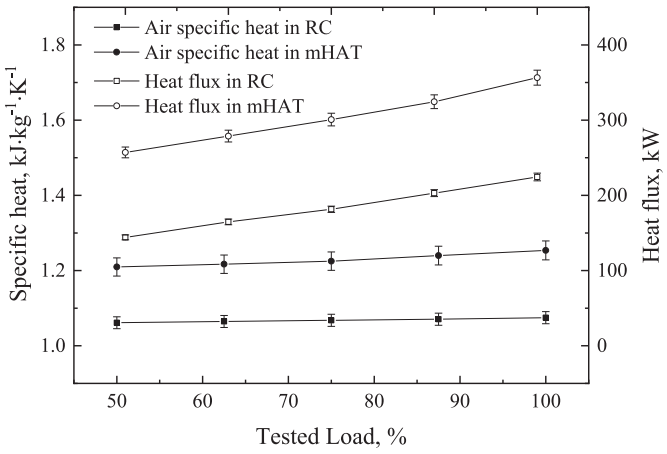

Fig. 17. Air specific heat and heat flux of recuperator in RC and mHAT.

Credit author statement

Zhen Xu, Conceptualization, Methodology, Investigation, Writing – original draft. Yuan Lu, Resources, Investigation, Data curation. Bo Wang: Software, Methodology, Validation. Lifeng Zhao, Data curation, Writing – review & editing. Yunhan Xiao, Project administration.

Declaration of competing interest

The authors declare that they have no known competing

financial interests or personal relationships that could have appeared to influence the work reported in this paper.

Acknowledgments

The authors would like to acknowledge the financial support by National Science and Technology Major Project (2017-I-0009-0010) to this research work.

Nomenclature

d	humidity ratio ($kg \cdot kg^{-1}$)
h	specific enthalpy ($kJ \cdot kg^{-1}$)
H	enthalpy rate (kJ)
G	volume flow rate of fuel ($m^3 \cdot s^{-1}$)
m	mass flow rate ($kg \cdot s^{-1}$)
n	number of combustible composition
P	absolute pressure (kPa)
Q	heating value of fuel ($kJ \cdot m^3$)
T	temperature of stream
w	specific output power (kW)
W	component work (kW)

Greek letters

β	pressure loss coefficient
ε	effectiveness of heat exchanger
η	electrical efficiency
ϕ	volume percentage

Subscripts

a	air
c	cold stream
da	dry air
d_f	dry flue gas
f	front
h	heat stream
i	inlet
id	ideal condition
j	composition number
LHV	low heating value
max	maximum
net	net
o	outlet
p	pumping work
r	compressor work
w	water
wb	wet bulb

References

[1] Ertesvåg IS, Kvamsdal HM, Bolland O. Exergy analysis of a gas-turbine combined-cycle power plant with precombustion CO_2 capture. Energy 2005;30(1):5–39.
[2] Ibrahim TK, Mohammed MK, Awad OI, Abdalla AN, et al. A comprehensive review on the exergy analysis of combined cycle power plants. Renew Sustain Energy Rev 2018;90:835–50.
[3] Rao AD. Process for producing power. US Patent; 1989. p. 4829763.
[4] Nakhamkin M, Swensen EC, Gaul G, Polsky M. The cascade humidified advanced turbine. J Eng Gas Turbines Power 1996;118(3):565–71.
[5] Yan J, Eidensten L, Svedberg G. Externally fired Evaporative Gas Turbine with a condensing heat exchanger. Proceedings of ASME turbo expo 1996;96. GT-77.
[6] Ågren N, Westermark MOJ. Design study of part-flow evaporative gas turbine cycles: performance and equipment sizing—partII: industrial core. J Eng Gas Turbines Power 2003;125(1):216–27.
[7] Jonsson M, Yan J. Economic assessment of evaporative gas turbine cycles with optimized part flow humidification systems. Proceedings of ASME turbo expo 2003:1–10. GT2003-38009.
[8] Dodo S, Nakano S, Inoue T, Ichinose M, et al. Development of an advanced microturbine system using humid air turbine cycle. Proceedings of ASME turbo expo 2004:167–74. GT2004-54337.
[9] Olaleye AK, Wang M. Techno-economic analysis of chemical looping combustion with humid air turbine power cycle. Fuel 2014;124:221–31.
[10] Hu Y, Li H, Yan J. Techno-economic evaluation of the evaporative gas turbine cycle with different CO_2 captures options. Appl Energy 2012;89:303–14.
[11] Zhao P, Dai Y, Wang J. Performance assessment and optimization of a combined heat and power system based on compressed air energy storage system and humid air turbine cycle. Energy Convers Manag 2015;103:562–72.
[12] Chacartegui R, Becerra JA, Blanco MJ, Muñoz-Escalona JM. A humid air turbine-organic rankine cycle combined cycle for distributed microgeneration. Energy Convers Manag 2015;104:115–26.
[13] Agren N, Westermark M, Bartlett M, Lindquist T. First experiments on an Evaporative Gas Turbine pilot power plant: water circuit chemistry and humidification evaluation. Proceedings of ASME turbo expo 2000;2:2000-GT-0168. No.2000-GT-0168,.
[14] Araki H, Higuchi S, Koganezawa T, et al. Test results from the advanced humid air turbine system pilot plant: Part 2—Humidification, water recovery and water quality. Proceedings of ASME turbo expo 2008;2:701–12. GT2008-51089.
[15] Takeda T, Araki H, Iwai Y, Morisaki T, Sato K. Test results of 40MW-class advanced humid air turbine and exhaust gas water recovery system. Proceedings of ASME turbo expo 2014;3A:GT2014-27281.
[16] Jonsson M, Yan J. Humidified gas turbines—a review of proposed and implemented cycles. Energy 2005;30:1013–78.
[17] J. Parente, A. Traverso, A. F. Massardo. Micro humid air cycle, Part A: thermodynamic and technical aspects. ASME paper, No. GT2003-38326.
[18] De Paepe W, Contino F, Delattin F, Bram S, De Ruyck J. Optimal waste heat recovery in micro gas turbine cycles through liquid water injection. Appl Therm Eng 2014;70(1):846–56.
[19] Nikpey H, Mansouri Majoumerd M, Assadi M, Breuhaus P. Thermodynamic analysis of innovative microturbine cycles. Proceedings of ASME turbo expo 2014;GT2014–26917. V03AT07A029.
[20] Paepe WD, Contino F, Delattin F, Bram S, Ruyck JD. New concept of spray saturation tower for micro humid air turbine applications. Appl Energy 2014;130:723–37.
[21] W. D. Paepe, M. Montero Carrero, S. Bram, F. Contino. T100 micro gas turbine converted to full humid air operation: test rig evaluation. ASME paper, No GT2014-26123.
[22] Wei C, Zang S. Experimental investigation on the off-design performance of a small-sized humid air turbine cycle. Appl Therm Eng 2013;51:166–76.
[23] Thern M, Lindquist T, Torisson T. Theoretical and experimental evaluation of a plate heat exchanger aftercooler in an evaporative gas turbine cycle. Proceedings of ASME turbo expo 2003;3:103–11. GT2003-38099.
[24] Zhang S, Xiao Y. Steady-state off-design thermodynamic performance analysis of a humid air turbine based on a micro turbine. Proceedings of ASME turbo expo 2006;5:287–96. GT2006-90335.
[25] Xu Z, Lu Y, Xiao Y. Experimental study on performances of a Micro-humid air turbine cycle. Proceedings of the CSEE 2012;32(35):1–5.
[26] Bowman Power. TG80 MK I version 3 installation manual. Document No. 9950-020.
[27] Pezzini P, Tucker D, Traverso A. Avoiding compressor surge during emergency shut-down hybrid turbine systems. J Eng Gas Turbines Power 2013;135(10):102602.
[28] Carrero MM, Ferrari ML, Paepe W De. Transient simulations of a T100 micro gas turbine converted into a micro humid air turbine. Proceedings of ASME turbo expo 2015;3:GT2015-43277.
[29] Bhargava A, Colket M, Sowa W, Casleton K, Maloney D. An experimental and modelling study of humid air premixed flames. J Eng Gas Turbines Power 2000;122:405–11.
[30] Xu Z, Xie Y, Xiao Y. A compact packing humidifier for the micro humid air turbine cycle: design method and experimental evaluation. Appl Therm Eng 2017;125:727–34.
[31] Xu Z, Lu Y, Zhao L, et al. Experimental evaluation of 100 kW grade micro humid air turbine cycles converted from a microturbine. Energy 2019;175:687–93. N.
[32] Ågren. Simulation and design of advanced air-water mixture gas turbine cycles. Technical Report. Royal Institute of Technology; 1997. ISRN/KET/R-74-SE.
[33] McCabe WL, Smith JC, Harriott P. Unit operations of chemical engineering. seventh ed. New York (USA): McGraw Hill; 2005.
[34] Xie Y, Zu Z, Mei N. Evaluation of the effectiveness-NTU method for countercurrent humidifier. Appl Therm Eng 2016;99:1270–6.
[35] Göke S, Schimek S, Terhaar S, Reichel TG. Influence of pressure and steam dilution on NOx and CO emissions in a premixed natural gas flam. J Eng Gas Turbines Power 2013;136(9):091508.
[36] De Paepe W, Sayad P, Bram S, et al. Experimental investigation of the effect of steam dilution on the combustion of methane for humidified micro gas turbine applications. Combust Sci Technol 2016;188(8):1199–219.
[37] Farokhipour A, Hamidpour E, Amani E. A numerical study of NOx reduction by water spray injection in gas turbine combustion chambers. Fuel 2018;212:173–86.
[38] Stevens T, Baelmans M. Optimal pressure drop ratio for micro recuperators in small sized gas turbines. Appl Therm Eng 2008;28:2353–9.